FAULT DETECTION AND ISOLATION IN PRESENCE OF INPUT AND OUTPUT UNCERTAINTIES USING BOND GRAPH APPROACH

Youcef TOUATI, Rochdi MERZOUKI, Belkacem OULD BOUAMAMA

Ecole Polytechnique de Lille, LAGIS, Boulevard Paul Langevin,
59655 Villeneuve d'Ascq Cedex, France

youcef.touati@polytech-lille.fr

ABSTRACT

In this paper, a bond graph model based approach for robust diagnosis in presence of input and output uncertainties is presented. Based on the structural and causal proprieties of the bond graph tool, a procedure of input and output uncertainties modeling is proposed in order to generalize the threshold generation. The proposed procedure is applied to the graphical model in preferred derivative causality, used for analytical redundancy relations. Simulation results are presented in order to validate the proposed procedure of thresholds and residuals generation.

Keywords: Robust fault detection and isolation, measurement uncertainty, Bond graph modeling.

1. INTRODUCTION

Robust fault diagnosis has been the subject of several researches in order to increase the sensibility of the diagnosis systems, to avoid false alarms and to insure the systems safety. Fault detection and isolation (FDI) is based essentially on the comparison between the real behavior of the system and a reference behavior describing the normal situation. The existing approaches to FDI in the literature can be classified on qualitative and quantitative approaches. Qualitative or non-model based methods, are principally based on the artificial intelligence and form recognition such as neuronal and Bayesian approaches (Hsing-Chia K. 2004), (Rothstein A. P. 2005). Qualitative or model based approaches, such as observers and parity relations, are based on the generation of residuals (Frank P.1990), (Iserman R. 1994). The latter are used as indicators in order to detect and isolate faults.In normal operation the residuals are close to zero and different from zero in faulty situations.

Several papers have been devoted to the FDI task in these last years. A survey of classical methods can be found in (Frank P. M. 1997). Many solutions to the robust diagnosis problem have been developed. For example, in (Casavola A. 2008), a solution to robust FDI problem is proposed using deconvolution filters (H_∞ and H_-) with a quasi-convex linear time invariant formulation.

In (Guo J. 2009), the author studied the robust fault detection filter design problem for linear time invariant (LTI) systems with unknown inputs and modeling uncertainties using the formulation of the robust fault detection filter design, as H_∞ model-matching problem, where a solution of the optimal problem is presented using the Linear Matrix Inequality (LMI) technique. Another approach has been developed using the parity space methodology (Han Z. 2002). In the latter, a new scheme of sensor and actuator fault detection and isolation for multivariate dynamic system in presence of parameter and measurement uncertainties is proposed. The measurement and parameter uncertainties are considered bounded and represented by bounded variables in the discrete time state space format.

Most of consulted papers try to eliminate the effect of the parameter or measurement uncertainties on the residuals, such as the filtering approach, which can cause the non-detection of certain faults. However, the parameter uncertainties is not associated to physical parameters but to the state matrix A. The bond graph can be an alternative for uncertainties modeling using the graphical representation. Furthermore, it is well suited for FDI. Indeed, the bond graph tool is used not only for modeling but also for diagnosis, due to its structural and causal proprieties. It is a unified graphical language for multi-physics domains (Karnopp D. 2000), (Borutzky W. 1999). The basic idea of diagnosis using bond graph approach is to generate the residuals, which represent the equations of energy conservation (junction equations), using directly the graphical model (Sueur C. 1991), (Low C. b. 2008). The causal proprieties of the bond graph are used to eliminate systematically the unknown variables, and the structural ones allow the generation of Analytical Redundancy Relations (ARR), using a covering causal paths methodology. The residuals are the evaluation of these ARRs and are used for real time diagnosis. More details about the structural proprieties of the bond graph model can be found in (Sueur C.1989).

2. BOND GRAPH THEORY

A bond graph $G(S,A)$ is a unified graphical language for multi-physic domains. Where the nodes S represent physical components, subsystems, and other basic elements called junctions. While the edges A, called power bonds represent the power exchanged between nodes.

The set of components named bond graph element is: $S = \{R \cup C \cup I \cup TF \cup GY \cup Se \cup Sf \cup De \cup Df \cup J\}$.

The R element represents a passive energy dissipation phenomena, while C, and I model the passive energy storage elements. (*Se*), and (*Sf*) are the sources of effort and flow, respectively. Sensors are represented by flow (*Df*), and effort (*De*) detectors. Finally, J (which can be a zero or a one junction), is used to connect the elements having the same effort (0 junction), or flow (1 junction). The conservative energy laws are obtained from the latter. *TF*, and *GY* are used to represent transformers and gyrators, respectively.

The passive elements are described by generic constitutive equations: dissipative R-elements (electrical resistor, hydraulic friction) are described by algebraic relationship $F_R(e,f) = 0$, potential storage energy C-element (capacitor, tank, spring) are modeled by an integral equation linking effort and integral of flow $\Phi_c\left(e,\int fdt\right)=0$ and kinetic storage energy I-element (mechanical inertia, electric coil) is quantified by integral equation between integral of effort and flow $\Phi_I\left(f,\int edt\right)=0$.

Definition Dualization of detectors is the replacing of the detector *De* and *Df* (Figure 1-a) by a signal source SSe and SSf respectively (Figure 1-b).

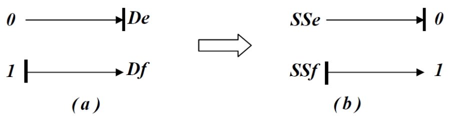

Figure 1: Dualization of detectors

Definition In a bond graph model, a causal path is an alternating of bonds and elements (*R, C, I*…) called nodes such that all nodes have a complete and correct causality. Causal paths of two bonds which have the same node have opposite causal direction. Depending on the causality, the passed variable is the effort or the flow. To change this variable, the causal path must pass through a junction element *GY*, or a passive element (*I*, *C* or *R*). Definition A system is under-constrained if its dynamic bond graph elements cannot accept the derivative causality when the detectors are dualized.

3. ROBUST FDI TO INPUT AND OUTPUT UNCERTAINTIES

3.1. Output uncertainty modeling

In this section, we describe a generalized method to model measurement uncertainties in order to generate uncertain *ARR*s, which can be used to obtain both residuals and thresholds. The dualized detectors on the bond graph model, used for diagnosis, in derivative causality impose the information signal to its associated junctions. Hence, the following equations can be obtained from Figure 2-(a) and (b), respectively:

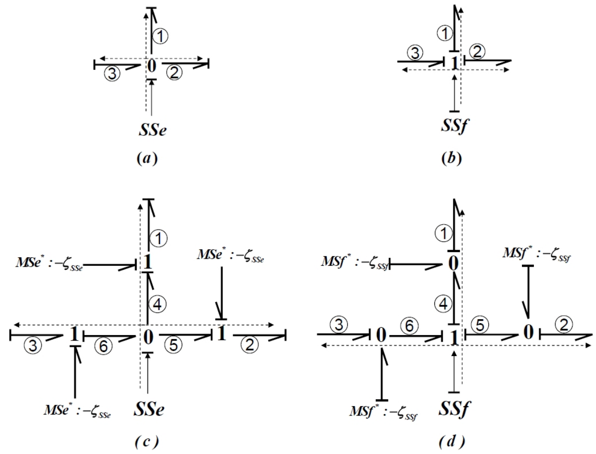

Figure 2: Measurement uncertainties modeling.

$$
\begin{aligned}
&(a)\begin{cases} e_1 = SSe; \\ e_2 = SSe; \\ e_3 = SSe; \end{cases} \\
&(b)\begin{cases} f_1 = SSf; \\ f_2 = SSf; \\ f_3 = SSf. \end{cases}
\end{aligned} \tag{1}
$$

The modeling of measurement uncertainties can be done as shown in Fig. 2-(c, d), which are based on the following equation (2):

$$
\begin{aligned}
&(c)\begin{cases} e_1 = e_4 - \zeta_{SSe} = SSe - \zeta_{SSe}; \\ e_2 = e_5 - \zeta_{SSe} = SSe - \zeta_{SSe}; \\ e_3 = e_6 - \zeta_{SSe} = SSe - \zeta_{SSe}; \end{cases} \\
&(d)\begin{cases} f_1 = f_4 - \zeta_{SSf} = SSf - \zeta_{SSf}; \\ f_2 = f_5 - \zeta_{SSf} = SSf - \zeta_{SSf}; \\ f_3 = f_6 - \zeta_{SSf} = SSf - \zeta_{SSf}. \end{cases}
\end{aligned} \tag{2}
$$

Where SSf and SSe represent the measured signal ζ_{SSe} and ζ_{SSf} represent the measurement error respectively on SSf and SSe.

3.2. Input uncertainty modeling

The inputs in bond graph tool are represented by a source of effort *Se*, or by a source of flow *Sf*, depending on the physical nature of the input components. As a mathematical point of view, the error on the inputs can be expressed as follow:

$$
\begin{cases} Se_r = Se + \zeta_{Se}; \\ Sf_r = Sf + \zeta_{Sf}. \end{cases}
$$

Where Se and Sf are the predicted input of the effort and flow source respectively, Se_r and Sf_r are the real effort and flow input. ζ_{Se} and ζ_{Sf} represent the uncertainties on the effort and flow source respectively.

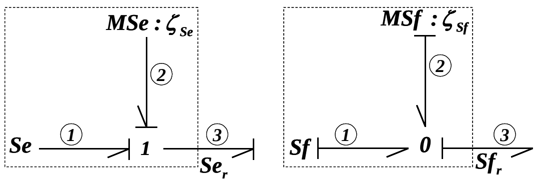

(a) (b)

Figure 3: **Input uncertainties modeling.**

This can be represented in a bond graph form as shown in Figure 3. For the ARR and threshold generation, the errors ζ_{Se} and ζ_{Sf} are considered bounded (3):

$$\begin{cases} -\Delta_{Se} \le \zeta_{Se} \le \Delta_{Se}; \\ -\Delta_{Sf} \le \zeta_{Sf} \le \Delta_{Sf}. \end{cases} \tag{3}$$

3.3. ARRs and thresholds generation

The thresholds generation can be done after the ARR generation using the following rules:

- Put the model in preferred derivative causality if possible.
- Model the measurement uncertainties directly on the bond graph model.
- Write the ARRs of the model using the equations of energy conservation, and use the causal path to eliminate the unknown variables.
- Write the ARRs of detectors redundancy.
- For all ARRs derived from the equations of energy conservation, the threshold is obtained by adding the maximal absolute values of the different parts of the ARRs containing the measurement errors.
- For the ARRs generated from the redundant detectors, the threshold is equal to the sum of the maximum measurement errors of the two redundant detectors.

Let us consider the linear system illustrated in Figure 4.

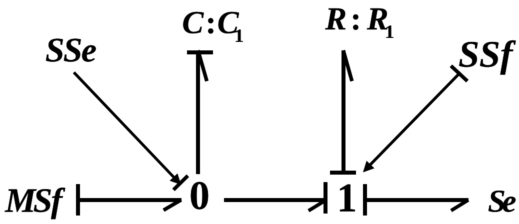

Figure 4: Linear system.

Two ARRs can be generated from this model, one from the 0-junction and the other from the 1-junction. The two ARRs are used as residuals, and theoretically equal to zero in normal situation, without considering the uncertainties and model errors. In presence of uncertainties on the sensors measurement, and if we know that the measurement error is an additive and bounded error, the residual can be bounded by a two thresholds, which can be calculated using the bond graph model directly. Applying the procedure of measurement uncertainties modeling, the model of the linear system become as shown in Figure 5. The model can be used to generate the uncertain part directly, by using the causal paths. For example in Figure 5: $MSf^*:\zeta_{Sf} \to 15 \to 3 \to 8 \to ARR_1$. These causal paths are used to generate the uncertain part of the ARR. We must start from virtual sources that represent the measurement errors to observed junctions (junctions which are connected to a detector). We remark that the virtual source of effort connected with the bond 13, and the virtual source of flow connected with the bond 7 have no causal path to an observed junction. So the measurement uncertainty on these bonds can be removed.

The measurement error on the bond 12 can be modeled directly on the observed junction like shown in Figure 6. This modeling procedure can be used with the R, C and I element connected to an observed junction. Using these rules the model of Figure 5 can be simplified to the model of Figure 7.

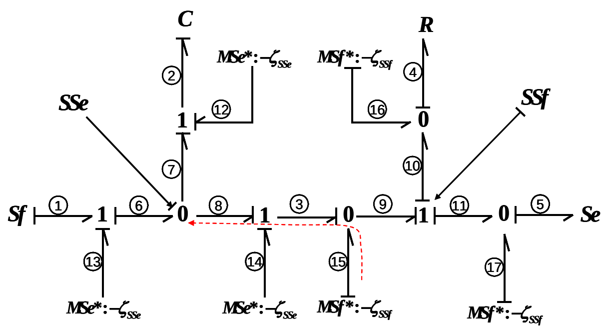

Figure 5: The model of the linear system with measurement uncertainties.

The robust ARRs of this system (Figure7) can be written as follows:

$$ARR_1 : MSf - C_1\frac{dSSe}{dt} - SSf + \zeta_{SSf} + \Phi_{C_1}\left(\zeta_{SSe}\right) = 0;$$

$$ARR_2 : SSe - R_1 SSf - Se + \zeta_{SSe} + \Phi_{R_1}\left(\zeta_{SSf}\right) + \Delta_{Se} = 0.$$

These two ARR can be decomposed to two residuals r_1 and r_2 (equation 4), and two thresholds a_1 and a_2 (equation 5).

$$\begin{aligned} r_1 &= MSf - C_1\frac{dSSe}{dt} - SSf; \\ r_1 &= SSe - R_1 SSf - Se. \end{aligned} \tag{4}$$

$$a_1 = max\left(\zeta_{SSf} + \Phi_{C_1}\left(\zeta_{SSe}\right)\right);$$
$$a_2 = max\left(\zeta_{SSe} + \Phi_{R_1}\left(\zeta_{SSf}\right) + \zeta_{Se}\right).$$

$$a_1 = max\left(\zeta_{SSf}\right) + max\left(\Phi_{C_1}\left(\zeta_{SSe}\right)\right);$$
$$a_2 = max\left(\zeta_{SSe}\right) + max\left(\Phi_{R_1}\left(\zeta_{SSf}\right)\right) + max\left(\zeta_{Se}\right). \quad (5)$$

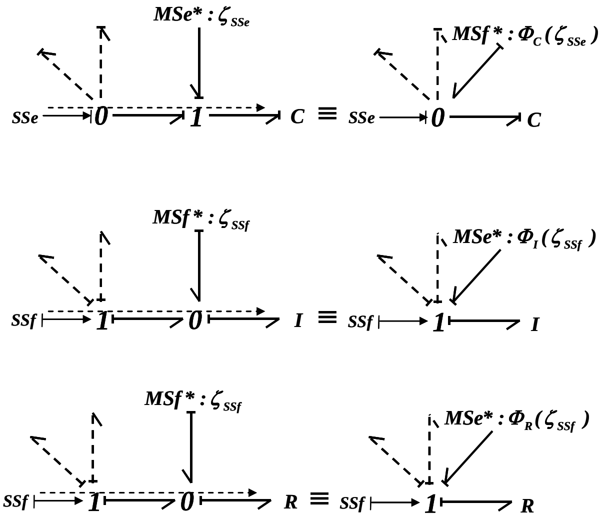

Figure 6: Simplification.

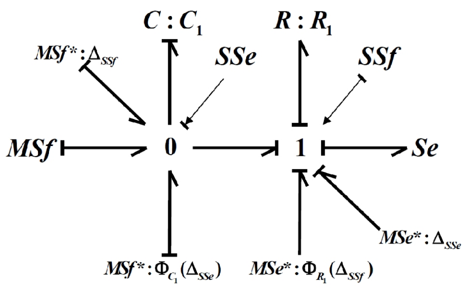

Figure 7: Simplified model of the linear system with measurement uncertainties.

$max\left(\Phi_{C_1}\left(\zeta_{SSe}\right)\right)$ can be bounded using the maximum and the minimum value of ζ_{SSe}.

$$max\left(\Phi_{C_1}\left(\zeta_{SSe}\right)\right) = max\left(C_1 \frac{d\zeta_{SSe}}{dt}\right).$$

In real applications, the differentiation is done in discrete time, by using some methods; the simplest is to use two values in different time as follows:

$$\frac{d\zeta_{SSe}}{dt} = \frac{\zeta_{SSe}^{i} - \zeta_{SSe}^{i-1}}{t_i - t_{i-1}}.$$

Where ζ_{SSe}^{i} is the measurement error in the time t_i. The measurement error is ζ_{SSe}^{i} bounded by Δ_{SSe}, so the quantity $\frac{\zeta_{SSe}^{i} - \zeta_{SSe}^{i-1}}{t_i - t_{i-1}}$ can be bounded as follows:

$$\frac{\zeta_{SSe}^{i} - \zeta_{SSe}^{i-1}}{t_i - t_{i-1}} \leq \frac{\Delta_{SSe} - \Delta_{SSe}}{t_i - t_{i-1}} \leq \frac{2\Delta_{SSe}}{t_i - t_{i-1}}.$$

So we can write:

$$max\left(\Phi_{C_1}\left(\zeta_{SSe}\right)\right) = C_1 \frac{2\Delta_{SSe}}{t_i - t_{i-1}}.$$

4. ROBUST FAULT ISOLATION

The fault isolation can be done using the fault signature matrix (*FSM*), which can be directly deduced either from the analytical redundancy relations or from the bond graph model directly, noting that the ARRs can be deduced directly from the graphical model. In this section, we propose a

Robust FSM (*S*) shown in Table I, where the columns are the residuals (r_i, $i = 1, 2,\ldots,n$), and the rows are the parameters that model the components (c_i, $i = 1, 2, \ldots m$).

Table 1:ROBUST FAULT SIGNATURE MATRIX.

	r_1	r_1		r_n	I_b	D_b
c_1	$s_{1,1}$	$s_{1,2}$	$\cdots$	$s_{1,n}$	g_1	e_1
c_2	$s_{2,1}$	$s_{2,2}$	$\cdots$	$s_{2,n}$	g_2	e_2
$\vdots$	$\vdots$	$\vdots$	$\vdots$	$\vdots$	$\vdots$	$\vdots$
c_m	$s_{m,1}$	$s_{m,2}$	$\cdots$	$s_{m,n}$	g_m	e_m

The $S^{m\times n}$ is a Boolean matrix, where:

$$\begin{cases} 1 \text{ if the } i^{th} \text{ ARR contains } c_j. \\ 0 \text{ otherwise.} \end{cases}$$

G is defined as the isolability vector, where:

$$\begin{cases} 1 \text{ if } s_{i,j=1 \text{ to } n} \text{ is unique,} \\ 0 \text{ otherwise.} \end{cases}$$

If the signature of the fault is unique, then the fault is isolable when its effect on the residuals is bigger than all the thresholds associated with these residuals.

E is the detectability vector calculated as follows:

$$e_i = s_{i,1} \vee s_{i,2} \vee \cdots \vee s_{i,n}.$$

The fault is detectable when its effect on the residuals is bigger than one of the sensible residual,

5. APPLICATION

In this section, the presented procedure of robust ARRs generation with respect to output and input uncertainties is applied to an electromechanical subsystem of a robot named Robotino. The latter is composed of three electromechanical subsystems (three omni-directional wheels with three DC motors). Each Subsystem contains two detectors that measure the current and the angular speed of the DC motor.

5.1. Modeling

The considered subsystem is modeled by bond graph tool as shown in Figure 8. To obtain the model, the different physical components and phenomenon are considered. The electrical part of the *DC* motor is modeled by R_a, L_a and U which represent the electrical resistance, inductance and the voltage, respectively. The energy transfer between the electrical part and the mechanical part (mechanical resistance R_e and inertia J_e) of the *DC* motor is represented by a gyrator (*GY*). The reducer is modeled by a transformer *TF* and the inertia of the wheel is represented by J_s and the resistance with R_s.

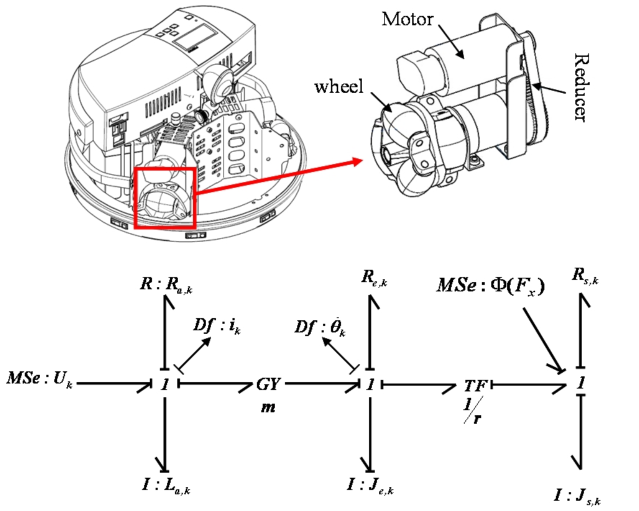

Figure 8: Bond graph model of the electromechanical subsystem.

From the model of Figure 9, the following ARRs can be obtained:

$$ARR_1 = U - L_a \frac{di}{dt} - R_a i - m \cdot \dot{\theta}_m + a_1;$$

$$ARR_2 = mi - J_e \frac{d\dot{\theta}_m}{dt} - R_e\dot{\theta}_m - \frac{J_s}{r^2}\frac{d\dot{\theta}_m}{dt} - \frac{R_s}{r^2}\dot{\theta}_m + \frac{1}{r}\Phi(F_x) + a_2;$$

$$a_1 = -\zeta_{R_a|i} - \zeta_{L_a|i} - m\zeta_{\dot{\theta}_m};$$

$$a_2 = -m\cdot\zeta_i - \zeta_{R_e|\dot{\theta}_m} - \zeta_{J_e|\dot{\theta}_m} - \frac{J_s}{r^2}\frac{d\zeta_{\dot{\theta}_m}}{dt} - \frac{R_s}{r^2}\zeta_{\dot{\theta}_m} + \frac{1}{r}\zeta_{\Phi(F_x)};$$

With

$$\zeta_{R_a|i} = \Phi_{R_a}(\zeta_i) = R_a\zeta_i;$$

$$\zeta_{L_a|i} = \Phi_{L_a}(\zeta_i) = R_a\frac{d\zeta_i}{dt};$$

$$\zeta_{R_e|\dot{\theta}_m} = \Phi_{R_e}\left(\zeta_{\dot{\theta}_m}\right) = R_e\zeta_{\dot{\theta}_m};$$

$$\zeta_{J_e|\dot{\theta}_m} = \Phi_{J_e}\left(\zeta_{\dot{\theta}_m}\right) = R_e\frac{d\zeta_{\dot{\theta}_m}}{dt}.$$

Where ζ_i and $\zeta_{\dot{\theta}_m}$ are the measurement errors on the current and velocity detectors respectively. $\zeta_{\Phi(F_x)}$ is the error on the input of the impact effort torch $\Phi(F_x)$, All the output and the input errors are considered bounded as follows:

$$|\zeta_i| \le 0.01A;\ \left|\zeta_{\dot{\theta}_m}\right| \le 0.1 rad/s;\ \left|\zeta_{\Phi(F_x)}\right| \le 0.001Nm;$$

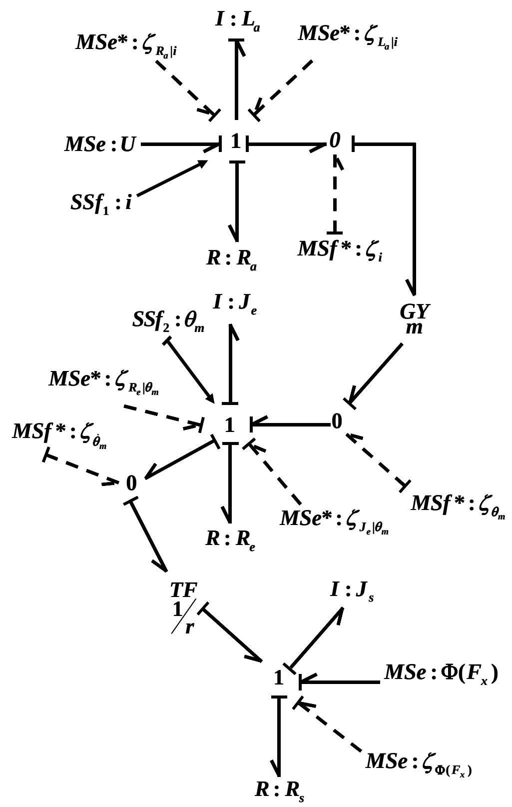

Figure 9: Bond graph model of the electromechanical subsystem with input

5.2. Simulation

In this subsection, simulations are performed in order to validate the developed diagnosis procedure in presence of input and output (measurement) uncertainties. The parameters (Table 2) of the model are obtained from a real system. The torque of the impact effort $\Phi(F_x)$ is considered as a constant and a bounded variable. The used sampling interval time is 0.2s.

Table 2: Parameters.

$$\begin{array}{l|l}
L_a & = 8.9mH \\
R_a & = 8.13\Omega \\
m & = 43.1mV \\
R_e & = 47\mu Nm.sec.rad^-1 \\
J_e & = 7.95 \times 10^-6Kg.m^2 \\
r & = 16 \\
J_s & = 63 \times 10^-3Kg.m^2 \\
R_s & = 0.02Nm.sec.rad^-1
\end{array}$$

Fig. 10 shows the input voltage signal, the output current of the electrical part of the system, and the output signal of the velocity of the wheel. In Fig. 11, the residuals and thresholds are represented. In Fig. 12, the residuals in faulty case are presented, where the additive fault on the input signal is around 12 %.

As the results show, the threshold depends on the precision of the detector and parameter values, and we remark that the derivative of the signal amplifies the noise. Consequently the thresholds also increase, because the estimation of the derivative depends on the sampling time.

6. CONCLUSION

In this paper, a procedure of robust fault detection and isolation using the bond graph tool is proposed, toward output (measurement) and input uncertainties, in order to avoid false alarms. This approach clearly shows that the performance of the diagnosis system depends on the sensors and actuators precision. In this graphical approach, the measurement and input uncertainties are associated, to the sensors (*Df* and *De*) and actuators (*Se, Sf*) respectively. In addition, this approach can be generalized and automated for *LTI* systems and some nonlinear systems.

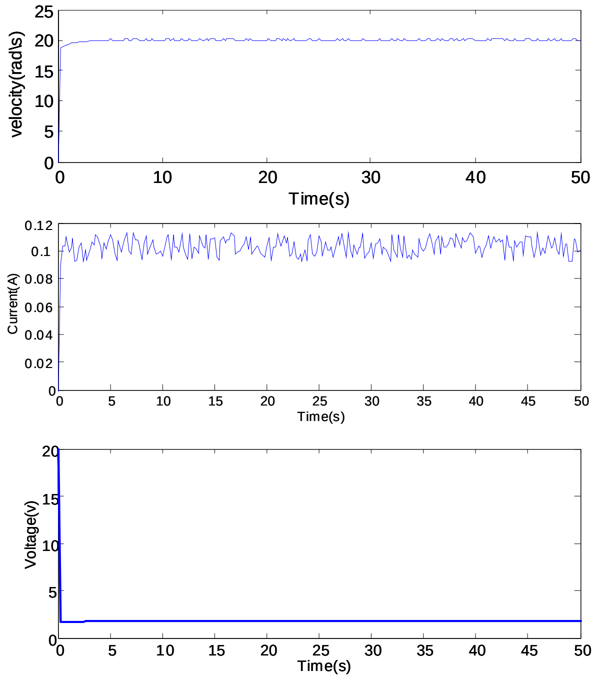

Figure 10: Voltage, current and velocity signals.

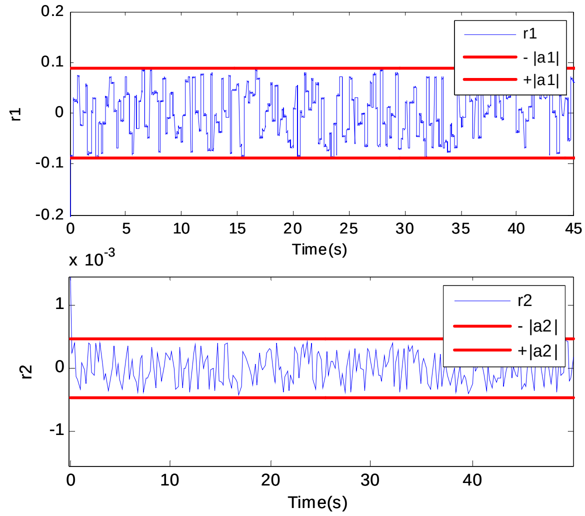

Figure 11: Residuals in normal situation.

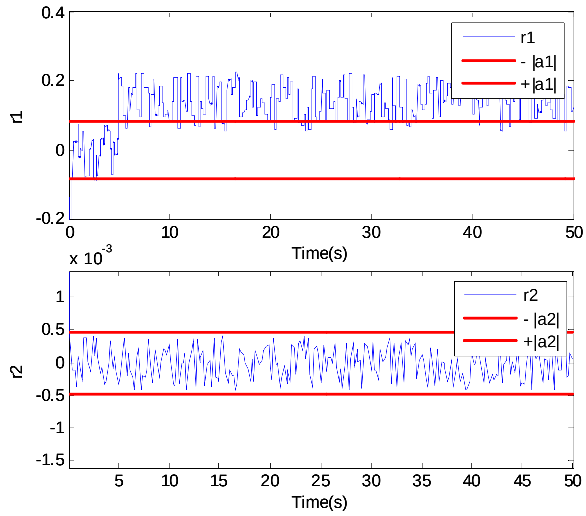

Figure 12: Residuals in faulty situation.

REFERENCES

Hsing-Chia K., Hui-Kuo C. 2004. ”A newsymbiotic evolution-based fuzzyneural approach to fault diagnosis of marine propulsion systems”. Engineering Applications of Arti cial Intelligence,Vol.17. pp. 919-930.

Rothstein A. P., Posner M., Rakytyanska H.B. 2005. ”Cause and effect analysis by fuzzy relational equations and a genetic algorithm”. Reliability Engineering and System Safety.

Frank P., 1990 “Fault diagnosis in dynamic systems using analytical and knowledge-based redundancy-a survey and some new results”, Automatica26 (3), 459-474.

Iserman R., 1994 Fault Detection based on modelling and estimation methods, a survey, Automatica 20 387-404.

Frank P. M. and Ding X. 1997 “Survey of robust residual generation and evaluation methods in observer- based fault detection systems” J. Proc. Cont. Vol. 7, N°. 6, pp. 403-424. Elsevier Science

Ltd.
Casavola A., Famularo D., Franz G. 2008, “Robust fault detection of uncertain linear systems via quasi-LMIs”. Automatica 44 289 - 295.
Guo J., Huang X., Cui Y., 2009 “Design and analysis of robust fault detection filter using LMI tools”. Computers and Mathematics with Applications 57 1743 1747.
Z. Han ,W. Li , S. L. Shah. 2002. “Fault detection and isolation in the presence of process uncertainties”. 15th IFAC Wold Congress. pp.1887-1892.
Karnopp D.C., Margolis D.L., Rosenberg R.C. , 2000 System Dynamics, Modeling and simulation of mechatronic systems. John Wiley and Sons Inc. ISBN 0-471-33301-8.
Borutzky W. , 1999, Relations between Graph based and object-oriented physical systems modeling, CBGM’99 International Conference on Bond Graph Modelling and Simulation, San Fransisco, CA, Jan. 17-20, pp.11-17.
Sueur C., Dauphin-Tanguy G., 1991, Bond graph approach for structural analysis of MIMO linear systems. J. Franklin Inst. 328 (1) 55-70.
Low C. B., Wang D., Arogeti S., Zhang J. B., 2008 Monitoring ability analysis and qualitative fault diagnosis using hybrid bond graph. Proceedings of the 17th World Congress The International Federation of Automatic Control Seoul, Korea, July 6-11.
Sueur C., Dauphin-Tanguy G. 1989. Structural Controllability and Observability of linear Systems Represented by Bond Graphs. Journal of Franklin Institute. Vol 326, Issue 6, 1989, Pages 869-883.